ISSN 1560-0904, Polymer Science, Ser. B, 2014, Vol. 56, No. 3, pp. 384–392. © Pleiades Publishing, Ltd., 2014.
Original Russian Text © I.V. Bakeeva, E.A. Egorova, N.S. Perov, I.V. Dementsova, E.V. Chernikova, V.P. Zubov, 2014, published in Russian in Vysokomolekulyarnye Soedineniya, Ser. B, 2014, Vol. 56, No. 3, pp. 343–352.

Magnetosensitive Organic–Inorganic Hybrid Hydrogels

I. V. Bakeeva[a],*, E. A. Egorova[a], N. S. Perov[b], I. V. Dementsova[b], E. V. Chernikova[b], and V. P. Zubov[a]

[a] *Moscow University of Fine Chemical Technology, pr. Vernadskogo 86, Moscow, 119571 Russia*

[b] *Faculties of Chemistry and Physics, Moscow State University, Moscow, 119991 Russia*

**e-mail: ir_bak@mitht.ru*

Received October 7, 2013;
Revised Manuscript Received January 27, 2014

Abstract—Magnetosensitive materials—organic–inorganic hybrid gels of the composition poly(*N*-vinylpyrrolidone)–silica nanoparticles–magnetite nanoparticles—whose native forms contain more than 80 wt % water are synthesized. Their magnetic and physicomechanical properties are studied, and the dependences of magnetization, shear modulus, and equilibrium degree of swelling are examined. It is shown that the type of magnetite nanoparticles and their amount determine the characteristics of hybrid-gel networks and affect the properties of the material.

DOI: 10.1134/S1560090414030038

INTRODUCTION

One of the ways to create new polymer materials with a set of desired characteristics is to modify polymers with additives of macrodispersed fillers or nanosized objects. The latter substances are preferred in modern studies and technologies [1]. The introduction of small amounts of nanofillers promotes changes in the initial properties and the appearance of new properties of polymer matrices. Nanoobjects influence the supramolecular packing of polymer macromolecules, a circumstance that affects the general properties of nanocomposite materials (NCMs).

Organic–inorganic hybrid hydrogels (OIHHs) with large amounts of immobilized water (hybrid hydrogels) may be classed with NCMs. The network of an OIHH comprises an organic polymer and inorganic nanoparticles. The type of bonds uniting components into a common three-dimensional structure depends on the presence of functional groups in polymer units and the surface features of nanoparticles. The organic polymer imparts improved physicomechanical properties combined with easy molding of articles into the hybrid material and, in some cases, the ability to reversibly respond in a desired manner to such factors as temperature, pH of the medium, a change of solvent, and the addition of a new cosolute [2]. Inorganic nanoparticles strengthen OIHHs; make them sensitive to pH [3, 4] and temperature [5]; provide marked magnetization in an external magnetic field [6–8]; and cause the appearance of peculiar fluorescent, optical, and catalytic properties [9–12]. For OIHHs to be advantageously used in biology and medicine, they should possess features typical for hydrogels (bioinertness, the ability to assume and keep any specified shape, the ability to absorb and retain solutes, etc.) and an additional, sensitive behavior in response to an external disturbing effect.

The goal of this study is to prepare and characterize magnetosensitive organic–inorganic hybrid hydrogels (MOIHHs) in which poly(*N*-vinylpyrrolidone) (PVP), silica (SiO_2) nanoparticles, and magnetic nanoparticles serve as gelling components. In the applied aspect, such MOIHHs are of interest for the creation of "soft" manipulators and as matrices for the delivery and controlled release of drugs. These compounds are also of interest for science as another type of OIHHs with the functional specificity. For example, the PVP–SiO_2 OIHH [13] was used as a matrix for immobilization and conservation of the properties of nanocrystalline silicon [14]. It was shown that a new material containing the nanocrystalline silicon is distinguished from the initial compound (PVP–SiO_2) in terms of its optical characteristics; that is, it can absorb light in the wavelength range 400–1000 nm.

Some inorganic compounds may be used as magnetic fillers [15], but iron oxides are the most suitable and sample for laboratory synthesis. Among them, magnetite (Fe_3O_4) is notable for the highest saturation magnetization and as the most commonly used component of magnetosensitive materials.

The synthesis of nanoparticles always poses challenges related to their stabilization. This problem may be resolved with the use of polymer molecules [16, 17]; in this study, PAA was used for this purpose. It is known that the adsorption of PAA on the surfaces of nanoparticles may ensure the colloid stabilization of magnetite nanoparticles [18, 19]. Preliminary experiments showed that the use of commercial oligomeric PAA ($M_n = 11.9 \times 10^3$ and $M_w/M_n = 1.78$) leads to the disturbance of crystallinity and partial oxidation of

Table 1. Characteristics of nanoparticles (the concentration of nanoparticles was 1.0 wt % in an aqueous dispersion)

Sample	pH	d, nm	ζ potential, mV	Domain diameter, nm
NP-1	7.0	13.7 ± 4.2	−32.14	5.6
NP-2	4.0	75.0 ± 11.9	−36.03	5.7
NP-3	4.0	31.2 ± 4.2	−34.46	4.7

magnetite nanoparticles. In contrast, oligomeric PAA prepared through preseudoliving radical polymerization via the RAFT mechanism and containing thiocarbonate fragments facilitates better stabilization of magnetite nanoparticles. This difference is apparently associated with different surface activities of PAA samples prepared via different methods [20]. Similar observations were reported in the study of stabilization of various mineral particles under conditions of simple component mixing [21]. Therefore, PAA prepared via RAFT polymerization [20] was used in this study to stabilize magnetic nanoparticles.

EXPERIMENTAL

$FeCl_2 \cdot 4H_2O$ (Merck), $FeCl_3 \cdot 6H_2O$ (Merck), a 30% aqueous solution of ammonium hydroxide (Merck), and PVP with $M = 1.3 \times 10^6$ (ISP Ashland) were used as received.

Tetramethoxysilane (TMOS) (Merck) was distilled under atmospheric pressure, and a fraction with T_b = 121–122°C and $n_D^{20} = 1.3680$ was used.

Oligomers of acrylic acid, PAA-1 and PAA-2, were synthesized via RAFT polymerization in the presence of typical sulfur-containing RAFT agents: dibenzyl trithiocarbonate $CH_2C_6H_5–S–C(=S)–S–CH_2C_6H_5$ and cyanoisopropyl dithiobenzoate $PhC(=S)S–C–(CH_3)_2(CN)$. The synthesis procedure was described in [20]; the molecular-mass characteristics of the polymers were as follows: $M_n = 8.4 \times 10^3$ and M_w/M_n = 1.56 for PAA-1, and for PAA-2, $M_n = 15.9 \times 10^3$ and $M_w/M_n = 1.35$.

Solutions were prepared with the use of bidistilled water.

Synthesis of Magnetic Nanoparticles

Magnetite nanoparticles were synthesized via the Massart method [22]; at room temperature, ferrous chloride and ferric chloride ($Fe^{2+} : Fe^{3+} = 1.0 : 2.6$) in an aqueous medium were coprecipitated under the action of ammonia. The solutions of iron salts were mixed for 7 min on a magnetic stirrer. The stirring was continued, and 30% ammonia was added dropwise until the ammonia concentration in the mixture was 8 wt %. Stirring was continued for another 15 min. As a result, the transparent light yellow solution converted into a black dispersion of Fe_3O_4 (pH 12.0).

The magnetite nanoparticles used in further experiments were washed with the aid of magnetic separation, and the procedure was repeated three times. Each time, a new portion of distilled water taken in an amount equal to the weight of decanted liquid was poured over the precipitate, and the mixture was vigorously shaken. When washing was completed, the dispersion of magnetite nanoparticles NP-1 was allowed to stay in an ultrasonic bath for 10 min; the characteristics of the dispersions are summarized in Table 1.

The dispersions of magnetite nanoparticles NP-2 and NP-3 (Table 1) were prepared through the addition of the as-prepared dispersion of NP-1 (3 mL) to aqueous solutions of PAA-1 and PAA-2 (1 mL), respectively, and stirring was continued for another 15 min (1000 rpm). The concentration of PAA in the dispersions was 1.25 wt %.

Synthesis of Magnetosensitive Organic–Inorganic Hybrid Gels

The dispersion of magnetite nanoparticles (0–1.5 wt %) was added under stirring on a magnetic stirrer to a solution of PVP. After 15 min, when the visible homogeneous dispersion of nanoparticles throughout the volume was attained, TMOS was added under stirring (PVP : TMOS = 1.0 : 0.6, base-mol/ mol), and the whole mass was stirred for another 5 min. The concentration of PVP in each case was constant and equal to 10 wt %.

MOIHHs were formed from the obtained liquid mixtures in closed plastic reservoirs in the form of cylinders with a height of 1.5 cm and a diameter of 3.0 cm at room temperature for a week on an even horizontal surface. In accordance with the type of nanoparticles that were incorporated into MOIHHs, the samples of various series were designated MOIHH-1, MOIHH-2, and MOIHH-3.

The pH values of dispersions were measured on a ZIP pH-340 pH meter.

The sizes and ζ potentials of magnetite nanoparticles were measured via dynamic light scattering on a Beckman Coulter DelsaNano C instrument (United States).

The IR spectra of the samples were measured on a Bruker EQUINOX 55 FTIR spectrometer (Germany). Pellets were pressed from the mixture of a dried powdered sample and KBr (2-mg sample and 200 mg KBr).

X-ray powder-diffraction analysis was performed on a Shimadzu XRD-6000 diffractometer (Japan).

The field dependences of magnetization for NP samples, their aqueous dispersions (magnetic liquids), and MOIHHs were measured at room temperature on a LakeShore VSM Series 7407 vibrating magnetometer (United States) in fields up to 16 kOe.

The rheological behavior of MOIHHs was studied with the aid of a TA-Plus automated texture analyzer (Lloyd Instruments Ltd., United Kingdom) at room temperature and under normal atmospheric conditions. Shear moduli E were estimated from the linear sections of the stress–strain curves during penetration of the samples at a strain rate of 0.3 mm/min; the precision level was ±0.1 kPa. Measurements were performed until 30% strain was attained.

The swelling of MOIHH samples in excess water was studied at a temperature of 25 ± 1°C. For this purpose, a sample was placed on a porous glass filter in a temperature-controlled cell. Variation in weight was studied in such a manner that the first point was measured after 5 min, while all other points were measured at 10-min intervals. The measurements were finished when the weight of the sample achieved a constant (equilibrium) value. The sample was a cylinder with a diameter of 1 and a height of 1.1 ± 0.1 cm. The samples of native hybrid gels were dried via staying for 1 h in a desiccator packed with a water-absorbing agent ($CaCl_2$), and the residual water was removed under vacuum for 30 h at room temperature until attainment of constant weights, which were assumed to be the weights of the dry samples.

Degrees of swelling α were estimated via the formula $\alpha = (m_2 - m_1)/m_1$, where m_1 and m_2 are the weights of the dried MOIHH and swollen MOIHH, respectively.

RESULTS AND DISCUSSION

As was shown in [23], once the aqueous solutions of PVP and TMOS are mixed, the initially liquid system gradually transforms into a transparent homogenous elastic OIHH. The three-dimensional network of this physical gel appears as a result of sol–gel transformations of TMOS in the aqueous solution of PVP and the formation of intermacromolecular bonds between PVP chains and silica clusters. It was anticipated that the addition of a dispersion of magnetite nanoparticles to the initial solution of PVP, followed by the addition of TMOS, likewise would give rise to an OIHH containing evenly distributed nanoparticles. Owing to the presence of functional groups on the surfaces of magnetite nanoparticles, it was expected that these groups would interact with gel components and insert into the volume of the gel network and that, because the magnetite nanoparticles are supermagnetic (i.e., in the absence of an external magnetic field, the orientation of their magnetic moments fluctuates), OIHHs would acquire magnetosensitive properties.

Magnetic Properties of NPs and OIHHs

Nanosized objects have unusual physical and chemical properties; they have high capacities for adsorption and substantial interfaces [24, 16]. In order to avoid aggregation and sedimentation of magnetite nanoparticles during their addition to the solution of PVP and then during the synthesis of OIHHs and to preserve the superparamagnetic behavior inherent in magnetic nanoparticles, their good stabilization is required.

Two types of nanoparticles were prepared. The first type, NP-1, was synthesized in a strongly alkaline medium, which provided sufficient stabilization of nanoparticles via electrostatic repulsion [22]. The second type of particles, NP-2 and NP-3, was obtained by the interaction of NP-1 with oligomers of acrylic acid. (The surface activities of PAA-1 and PAA-2 were discussed in [20].) As is clear from Table 1, NP-2 and NP-3 are aggregates composed of several NP-1 particles covered with a polymer shell. PAA molecules are strongly adsorbed on the surfaces of nanoparticles via the interaction of both the carboxyl groups of oligomer molecules (PAA-1 and PAA-2) and the hydrophobic sulfur-containing fragments with the surfaces of nanoparticles; as a result, structural–mechanical barriers for the repulsion of particles are created. Moreover, the carboxyl groups of PAA units can form hydrogen bonds with the carbonyl groups of PVP units. This circumstance facilitates better compatibility of magnetite nanoparticles NP-2 and NP-3 with PVP during the formation of OIHHs. All dispersions of magnetite nanoparticles retain their characteristics for a month and after dilution with water (Table 1).

The X-ray patterns (Fig. 1) of the nanoparticles show peaks at diffraction angles 2θ typical for magnetite: 30.1°, 35.9°, 43.1°, 57.0°, and 62.6° (which correspond to the planes (220), (311), (400), (511), and (440)). The peaks are well-defined and feature pronounced intensity. With the use of the characteristic peaks at 2θ of 57.0° and 62.6°, the approximate diameters of magnetite nanoparticles were calculated via the Scherrer formula [25] (Table 1). On the basis of X-ray diffraction data, it may be inferred that, in all samples, the magnetite phase prevails and nanoparticles are nanosized.

The interaction of the surfaces of magnetite nanoparticles with PAA is confirmed by FTIR spectroscopy (Fig. 2). In the spectra of NP-2, the absorption band at 1710 cm^{-1} (assigned to carboxyl groups) slightly shifts relative to the spectrum of PAA-1 and a new absorption band at 1590 cm^{-1} (typical for the anionic form of the carboxyl group) appears. In addition, unlike in the spectrum of NP-1, in the spectrum of NP-2, the absorption band corresponding to the magnetite hydroxyl (597 cm^{-1}) is shifted. This fact suggests that the surfaces of magnetite nanoparticles interact via coordination bonds with PAA macromolecules. Similar data were obtained for NP-3.

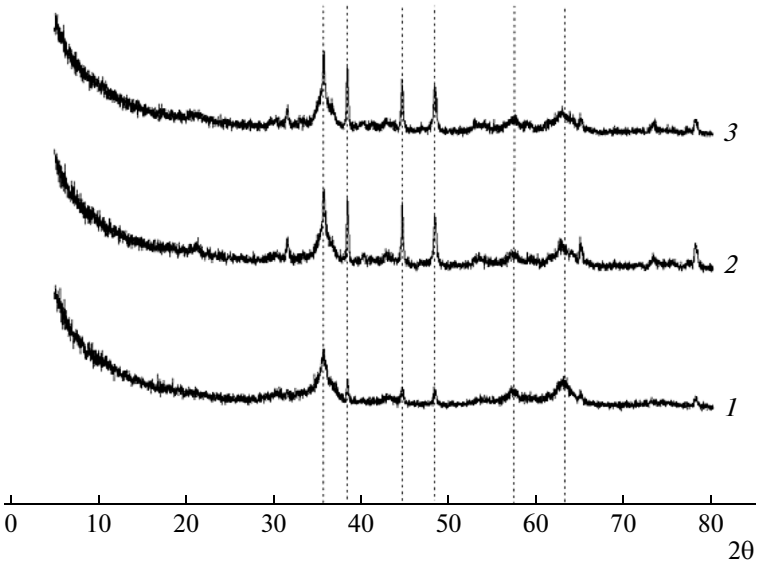

Fig. 1. X-ray patterns of (*1*) NP-1, (*2*) NP-2, and (*3*) NP-3 samples.

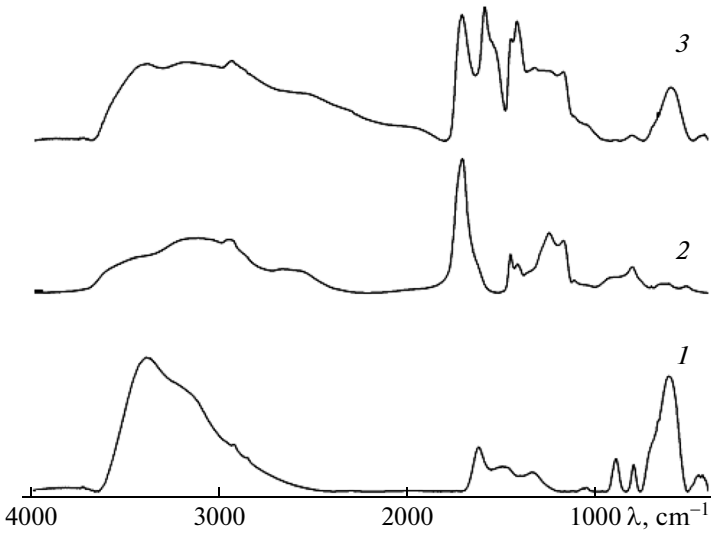

Fig. 2. IR spectra of (*1*) NP-1, (*2*) PAA-1, and (*3*) NP-2.

Test experiments showed that nanoparticles in an aqueous dispersion assembled against a point at which a magnet was applied from the outside; the remaining volume of the solution became fully transparent. The OIHHs containing more than 80 wt % water are magnetic-field-sensitive. A block native MOIHH could follow the magnet, but there was no separation of magnetite nanoparticles in the volume of the material, regardless of the magnet's position. After full removal of water from the MOIHH, the interaction of the sample with the magnet became more pronounced. In the case of neither native MOIHH samples nor dried samples, no magnetite nanoparticles appeared in the solution when they were placed in excess water and allowed to stay for 10 days; however, they preserved movement toward the magnet's side. Hence, the sizes of magnetite nanoparticles slightly change during the formation of MOIHHs and the particles retain initial properties, while OIHHs acquire sensitivity to the magnetic field.

In the maximum magnetic field (16 kOe), field dependences of magnetization were obtained for aqueous dispersions of nanoparticles and MOIHHs (Fig. 3). The magnetic characteristics of MOIHHs, dispersions of nanoparticles, and the same nanoparticles after full removal of water are listed in Table 2. Evolution in the character of the temperature dependence of magnetization during heating and cooling

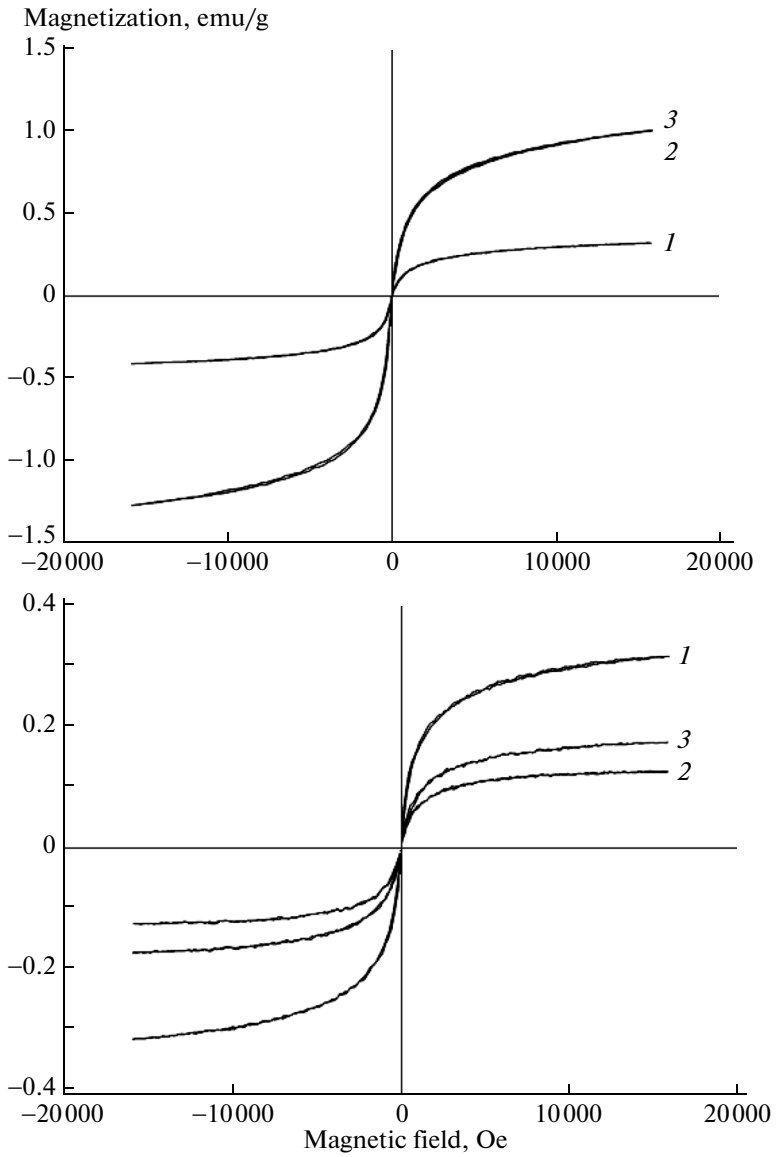

Fig. 3. Magnetization curves for aqueous dispersions of (a) magnetite nanoparticles and (b) native MOIHHs: (a) (*1*) NP-1, (*2*) NP-2, and (*3*) NP-3; (b) (*1*) MOIHH-1, (*2*) MOIHH-2, and (*3*) MOIHH-3.

makes it possible to state that the sizes of magnetite nanoparticles in MOIHHs are within 30–40 nm; these values are quite commensurable with their initial sizes (Table 1).

As is clear from Fig. 3a, all samples feature the superparamagnetic behavior because the curves do not plateau at the maximum intensity of the applied magnetic field (do not reach full saturation). In the case of superparamagnetic particles, the smaller the size of particles, the more difficult the arrangement of magnetic moments in parallel to the magnetic field [26]. For NP-2 and NP-3 samples, the magnetic moments of the supermagnetic fraction are higher; hence, effective volumes d of these nanoparticles are higher than that of NP-1 samples (Table 1). This finding indicates the efficient stabilization of magnetite nanoparticles by oligomeric PAA.

Different levels of magnetization of nanoparticles at the maximum intensity of the applied magnetic field (Table 2) may be explained by a change in the initial phase composition. If NP-1 samples are stabilized insufficiently, then partial oxidation of the magnetite surface into hematite, which possesses much less magnetization, will occur in an aqueous medium [27]; hence, the magnetization of NP-1 will be lower, as was the case in experiments.

In the case of dried nanoparticles, as is seen from Table 2, the magnetization of NP-1 is two times greater than that of NP-2 and NP-3, although smaller particles are less susceptible to magnetization than

coarser particles. In other words, NP-1 particles stick together during cooling and the electrostatic stabilizing factor weakens, whereas the efficiency of the polymer stabilizer is insensitive to the removal of water and the protective layer on nanoparticles remains unchanged. The coercive forces are almost the same for samples of each series and are independent of the method of nanoparticles stabilization (Table 2). The difference in coercive forces between the dispersions of nanoparticles and their dried analogs is related to the fact that, in an aqueous medium, particles may rotate relative to the field and the orientation of magnetic field may change in any field. In the dried state, the orientation of the magnetic moment may change owing to the magnetic reversal of particles only and the coercivity is determined by anisotropy of the material of the particles.

The magnetization of aqueous dispersions of magnetite nanoparticles is a factor of 7 greater than that of native MOIHH-2 and MOIHH-3 samples (Fig. 3). This circumstance may be explained by different concentrations of nanoparticles in the MOIHH samples (0.5 wt %) and in the aqueous dispersions (3 wt %). However, the quantitative data on the magnetization of MOIHH-1 and the dispersion of NP-1 are almost the same. The magnetization of MOIHHs containing NP-1 is a factor of almost 2 greater than the magnetization of MOIHHs containing NP-2 and NP-3; that is, the type of stabilization of nanoparticles shows a stronger effect of the magnetization of nanoparticles and the properties of OIHHs than the effect of the sizes of nanoparticles and their concentrations.

The sequence in the arrangement of the dependences shown in Fig. 3b may have several causes. If NP-1 particles enlarge during the formation of MOIHH-1, the magnetization of the sample increases. However, the coercive force of MOIHH-1 differs insignificantly from the coercive force of the corresponding magnetic liquid (Table 2). This result implies that the aggregation of nanoparticles is absent during the formation of MOIHHs. In this case, NP-1 may rotate almost freely in MOIHHs and arrange in the direction of the applied magnetic field. However, a hybrid gel is dense enough to limit the free rotation of nanoparticles within the gel and will exhibit a stronger effect on nanoparticles if they are incorporated into the network of the gel. Hence, the observed differences are possible only when NP-1 particles are not fixed in the walls of the gel. In contrast, NP-2 and NP-3 particles are structured in the network of the MOIHH. Therefore, it may be suggested that the network of gel MOIHH-1 differs from the networks of gels MOIHH-2 and MOIHH-3. This statement is indirectly confirmed by the physicomechanical study of MOIHHs.

As is seen from the above data, the properties of NP-1 both in the dried state and in MOIHHs differ appreciably from those of NP-2 and NP-3. This evidence may be rationalized by the presence of the protective polymer layers on the surfaces of nanoparticles.

Table 2. Magnetic characteristics of magnetite nanoparticles, dispersions of magnetite nanoparticles, and MOIHHs

Sample	Coercive force, Oe	Magnetization, emu/g
Dry NPs		
NP-1	114	27.50
NP-2	110	14.04
NP-3	110	13.20
Magnetic liquids		
NP-1	1.3	0.32
NP-2	1.6	0.96
NP-3	1.5	1.01
MOIHHs		
MOIHHs-1	1.0	0.32
MOIHHs-2	0.6	0.13
MOIHHs-3	0.7	0.16

Precisely this layer hampers the adhesion of nanoparticles during drying and hinders the rotation of nanoparticles incorporated into MOIHHs. Note that there is no marked difference in the properties of nanoparticles stabilized by PAA-1 and PAA-2. This result may be explained by the fact that both the formation and structure of PAA layers on the surfaces of magnetite nanoparticles are determined solely by the interaction of carboxyl groups of PAA with the hydroxyl groups on the surfaces of NPs; therefore, differences in PAA-1 and PAA-2 level off.

Physicomechanical Properties of MOIHHs

Because the compositions of the initial reagents used to prepare MOIHH samples were the same, the differences in their properties will primarily depend on the parameters of the gel networks (the types of junctions, their structuring, and their frequency). It is advisable to correlate these dependences with the pH of the medium and the type of magnetite nanoparticles used in gelation.

Dependences of the equilibrium degrees of swelling (Table 3) and shear moduli (Fig. 4) on the concentrations of magnetite nanoparticles in MOIHH samples were obtained.

All series of MOIHHs showed the same tendency during swelling in excess water: As the concentration of any of the magnetite nanoparticles increased, the absorption ability of the MOIHHs increased for both native forms and analogous predried samples. In every case, the kinetics of swelling showed similar features: The main changes in the rate of water entry occurred during the first 20 min; then, the degree of swelling gradually increased with time and attained the equilibrium value 150 min after the onset of the process.

The equilibrium degrees of swelling for native samples of the MOIHH-2 and MOIHH-3 series are on

Table 3. Equilibrium degrees of swelling of MOIHH samples

Magnetite		α, g/g	
NP type	[NP], wt %	native MOIHH	dried MOIHH
No*	0	5.56	0.93
NP-1	0.03	5.64	1.33
	0.25	5.85	1.44
	0.50	5.98	1.67
	1.00	6.90	2.78
	1.50	6.96	3.05
NP-2	0.03	7.05	1.35
	0.25	7.62	1.52
	0.50	8.81	1.78
	1.00	9.90	2.11
	1.50	10.52	2.18
NP-3	0.03	7.63	2.03
	0.25	7.93	3.06
	0.50	8.32	3.17
	1.00	8.73	3.29
	1.50	9.08	3.35

* OIHHs were formed at pH 7.0.

average 1.5 times higher than those for samples of MOIHH-1 and the OIHH (the gel lacking magnetite nanoparticles) (Table 3). It may be suggested that magnetite nanoparticles change the supramolecular packing of PVP chains and affect parameters of the gel network. A lower swelling ability of MOIHH-1 samples than those of other MOIHHs is probably related to structural differences between these samples.

As was shown in [28], during desorption of water from hybrid hydrogels, there are structural rearrangements that irreversibly change the native structures of the hydrogels. The unusual character of the formed primary structure of the OIHH and its lability were observed in [29], especially in the case of full dehydration during drying of such OIHHs. It was found [29] that the structuring of hybrid gels at the macro- and microlevels changes owing to some processes, including the aggregation of primary silica particles, which entails a decrease in the ability of the dried OIHH to swell in excess water. It appears that the evident distinctions in the equilibrium degrees of swelling (Table 3) for the native forms of MOIHHs and the forms of MOIHHs that were preliminarily dried have similar causes.

Variation in the shear moduli of MOIHH samples with the concentrations of magnetite nanoparticles (Fig. 4) depends on the type of nanoparticles to a higher extent than on their amounts. It was found that higher concentrations of the added magnetite nanoparticles in OIHHs led to stronger hydrogels. The effect of NP-1 incorporated into MOIHH-1 may be described as corresponding to the inactive filler that strengthens the material but does not affect the gel network at a "concentration of saturation" of nanoparticles of 1 wt %. As the concentrations of nanoparticles in MOIHHs increase further, shear moduli cease changing appreciably. For MOIHH-1, the modulus is almost two times higher than those for MOIHH-2 and MOIHH-3 in the concentration range of NPs up to 1 wt %. The only exception is the samples containing the highest amount of magnetite nanoparticles (1.5 wt %). In this case, the best characteristics are featured by MOIHH-2 and MOIHH-3.

Different "zero" points on Fig. 4 (4.3 and 2.0 kPa) correspond to the shear moduli of OIHHs measured at pH 7.0 and 4.5. Acidification of the PVP solution catalyzes sol–gel transformations of TMOS, thereby facilitating the acceleration of hydrolysis [30]. Depending on the acidity of the medium, silica particles with different morphologies form. This circumstance may affect the formation of the gel network and may be responsible for different strength characteristics of OIHHs (pH 4.5) and MOIHH-2 and MOIHH-3, especially in the samples containing less than 0.5 wt % nanoparticles.

During the formation of MOIHH-2 and MOIHH-3, the aqueous media have weakly acidic pH values because dispersions of NP-2 and NP-3 are among the used initial components. Note that the acidic groups are localized in the surface shells of these magnetite nanoparticles. It is not inconceivable that polyorganosiloxane chains will form in the immediate vicinity of the surfaces of magnetite nanoparticles and most probably will entwine them. The appearance of silica layers on the surfaces of NP-2 and NP-3 will affect their mobilities in the magnetic field and will additionally reduce the magnetization of MOIHH-2 and MOIHH-3 (Fig. 3b) relative to the magnetization obtained for analogous aqueous dispersions of nanoparticles.

The experiments were performed as follows: During mixing, TMOS was added dropwise to each dispersion of magnetite nanoparticles (the concentration of nanoparticles was 1 wt %) at a volume ratio of 1 : 3. After 5 min, the system containing NP-1 transformed into a dense but fragile hydrogel that easily crumbled under a small mechanical effect. In two other experiments, the systems remained homogeneous and viscous for a long time and analogous hydrogels formed only after 12 h. Three-dimensional structures in the presence of NP-2 and NP-3 form much slower, and there are processes that decelerate polycondensation and growth of branched silica chains connected over volume. In turn, the addition of magnetite nanoparticles at a concentration of 3 wt % into the solution of PVP and storage of these mixtures over time entailed neither gel formation nor an evident gain in the viscosity of the solution.

During the formation of MOIHH-2 and MOIHH-3, it may be expected that a "network-in-network" struc-

ture may form, because polyorganosiloxane chains interact with both PVP chains [23] and magnetite nanoparticles [17] and that the structure of the MOIHH-1 network is similar to that of the OIHH [23] with a small difference related to the presence of NP-1. On the basis of the above reasoning, the following structures of MOIHHs may be proposed.

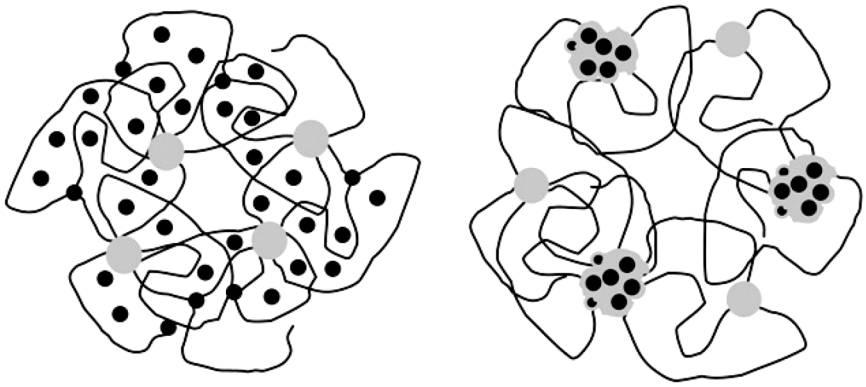

In MOIHH-1, silica particles (gray circles) occur in gel network junctions that link PVP macromolecules and form a common three-dimensional gel whose cells contain NP-1 (black circles); as a consequence, the packing of PVP macromolecules becomes looser. During preparation of mixtures used for the further formation of the hybrid material, NP-1 particles were preliminarily dispersed in the solution of PVP. It appears that, at this stage, the adsorption of fragments of PVP macromolecules on their surfaces occurred and the interaction of NP-1 particles with polyorganosiloxanes became impossible along with their incorporation into the gel network. As a result, magnetite nanoparticles were able to move in the gel, the strength of the whole material improved, and carbonyl groups in PVP units (sites of interaction between the hybrid-hydrogel matrix and water) became more accessible to water molecules.

For MOIHH-2 and MOIHH-3, not only silica nanoparticles (gray circles) but also united clusters, in which magnetite nanoparticles and silica component are located, serve as points of binding of PVP macromolecules. These clusters and fragments of PVP chains that occur within them are fragments of interpenetrating networks. As the amounts of magnetite nanoparticles in both MOIHH-2 and MOIHH-3

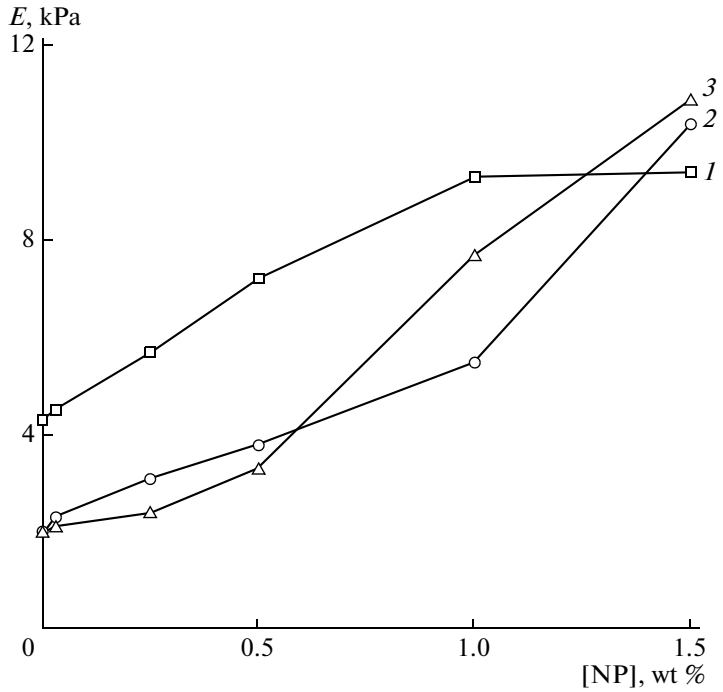

Fig. 4. Shear modulus vs. concentration of magnetite nanoparticles in (*1*) MOIHH-1, (*2*) MOIHH-2, and (*3*) MOIHH-3.

increase, larger amounts of silica are consumed in the formation of mixed-type junctions and the fraction of "traditional" junctions decreases, but their total effect provides for the formation of hybrid gels whose features are comparable with those of MOIHH-1.

The above structural schemes of MOIHHs explain the different magnetic and physicomechanical properties, namely, the tendency toward change in the values of magnetization, shear modulus, and equilibrium degree of swelling of MOIHH samples, depending on the type and amount of magnetite nanoparticles. In addition, these schemes give an idea on how variation in the surface layers of magnetite nanoparticles makes it possible to control the structuring of the gel networks and to obtain materials with desired characteristics.

ACKNOWLEDGMENTS

This work was supported in part by the Russian Foundation for Basic Research, project no. 13-02-90491.

REFERENCES

1. A. C. Balazs, T. Emrick, and T. P. Russel, Science (Washington, D. C.) **314**, 1107 (2006).
2. S. Nayak and L. A. Lyon, Angew. Chem., Int. Ed. Engl. **44**, 7686 (2005).
3. Y. Sun, Y. Liu, G. Zhao, X. Zhou, J. Gao, and Q. Zhang, J. Mater. Sci. **43**, 4625 (2008).
4. T. Zhang, Y. Wu, X. Pan, Z. Zheng, X. Ding, and Y. Peng, Eur. Polym. J. **45**, 1625 (2009).
5. A. P. Whittington, S. T. Nguyen, and J.-H. Kim, Nanoscape **6**, 26 (2009).
6. T.-Y. Liua, S.-H. Hua, K.-H. Liua, D.-M. Liub, and S.-Y. Chen, J. Magn. Magn. Mater. **304**, 397 (2006).
7. V. M. De Paoli, S. H. De Paoli Lacerda, L. Spinu, B. Ingber, Z. Rosenzweig, and N. Rosenzweig, Langmuir **22**, 5894 (2006).
8. A. T. Paulino, A. R. Fajardo, A. P. Junior, E. C. Munizo, and E. B. Tambourgi, Polym. Int. **60**, 1324 (2011).
9. C. Burda, X. Chen, R. Narayanan, and M. A. El-Sayed, Chem. Rev. **105**, 1025 (2005).
10. X. Wang, D. R. G. Mitchell, K. Prince, A. J. Atanacio, and R. A. Caruso, J. Chem. Mater. **20**, 3917 (2008).
11. L. Guo, Q.-J. Huang, X.-Y. Li, and S. Yang, Langmuir **22**, 7867 (2006).
12. S. S. Ivanchev and A. N. Ozerin, Polym. Sci., Ser. B **48**, 213 (2006).
13. Yu. O. Kirillina, Candidate's Dissertation in Chemistry (Moscow, 2009).
14. V. P. Zubov, A. A. Ishchenko, P. A. Storozhenko, I. V. Bakeeva, Yu. O. Kirilina, and G. V. Fetisov, Dokl. Chem. **437**, 120 (2011).
15. S. P. Gubin, Yu. A. Koksharov, G. B. Khomutov, and G. Yu. Yurkov, Usp. Khim. **74**, 539 (2005).
16. D. A. Baranov and S. P. Gubin, RENSIT **1**, 129 (2009).
17. A.-H. Lu, E. L. Salabas, and F. Schuth, Angew. Chem., Int. Ed. Engl. **46**, 1222 (2007).
18. S. Wei, Y. Zhang, and J. Xu, Colloids Surf. A **296**, 51 (2007).
19. J. Ge, Y. Hu, M. Biasini, C. Dong, J. Guo, W. P. Beyermann, and Y. Yin, Nanocrystals. Chem. Eur. J. **13**, 7153 (2007).
20. E. A. Egorova, V. P. Zubov, I. V. Bakeeva, E. V. Chernikova, and E. A. Litmanovich, Polym. Sci., Ser. A **55**, 519 (2013).
21. J. Loiseau, N. Doerr, J. M. Suau, J. B. Egraz, M. F. Llauro, and C. Ladaviére, Macromolecules **36**, 3066 (2003).
22. R. Massart, IEEE Trans. Magn. **17**, 1247 (1981).
23. Yu. O. Kirilina, I. V. Bakeeva, N. A. Bulychev, and V. P. Zubov, Polym. Sci., Ser. B **51**, 135 (2009).
24. A. D. Pomogailo, Usp. Khim. **66**, 750 (1997).
25. A. I. Kitaigorodskii, *X-Ray Diffraction Analysis of Finely Crystalline and Amorphous Bodies* (GITTL, Moscow, 1952) [in Russian].
26. X. Batlle and A. Labarta, J. Phys. D: Appl. Phys. **35** (6), R15 (2002).
27. D. Ortega, *Magnetic Nanoparticles: From Fabrication to Clinical Applications*, Ed. by N. T. K. Thank (CRC, New York, 2012).
28. G. S. Kulagina, V. K. Gerasimov, and A. E. Chalykh, Izv. Vyssh. Uchebn. Zaved., Khim. Khim. Tekhnol. **49** (2), 40 (2006).
29. I. V. Bakeeva, L. A. Ozerina, A. N. Ozerin, and V. P. Zubov, Polym. Sci., Ser. A **52**, 496 (2010).
30. R. Iler, *Chemistry of Silica* (Wiley, New York, 1979; Mir, Moscow, 1982), Vol. 1.

Translated by T. Soboleva